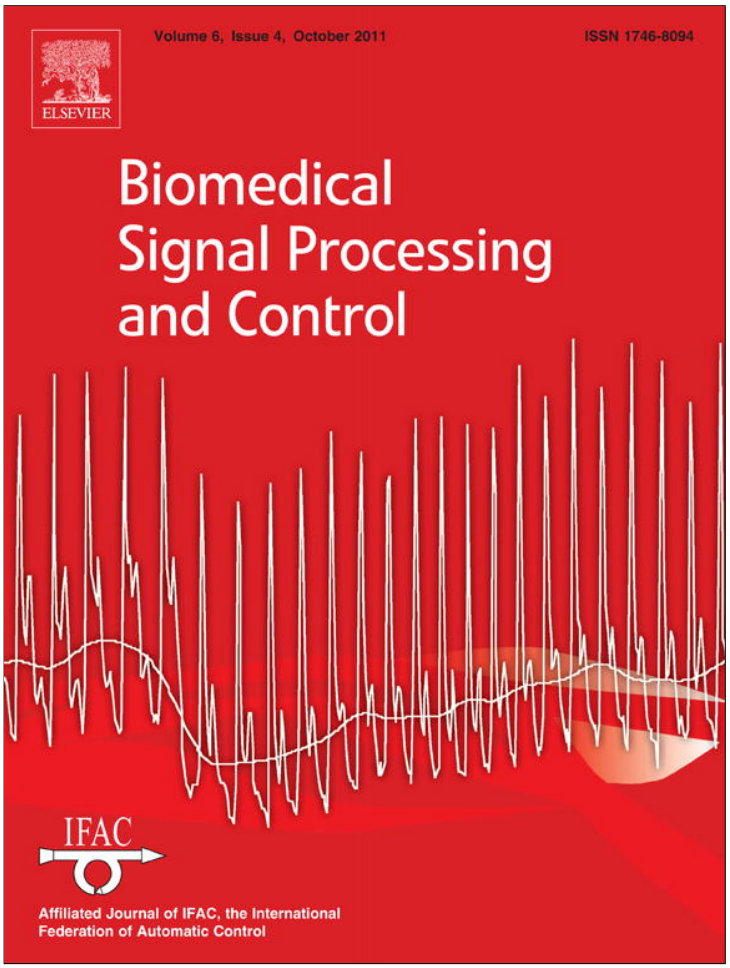

Biomedical Signal Processing and Control 6 (2011) 387–394

Contents lists available at ScienceDirect

Biomedical Signal Processing and Control

journal homepage: www.elsevier.com/locate/bspc

A two-dimensional approach for lossless EEG compression

K. Srinivasan[a,b,*], Justin Dauwels[b], M. Ramasubba Reddy[a]

[a] Biomedical Engineering Group, Department of Applied Mechanics, IIT Madras, Chennai 600036, India
[b] School of Electrical & Electronic Engineering, Nanyang Technological University, Singapore 639798, Singapore

ARTICLE INFO

Article history:
Received 27 April 2010
Received in revised form 17 January 2011
Accepted 17 January 2011
Available online 11 February 2011

Keywords:
Arithmetic coding
Correlation coefficient
Electroencephalogram (EEG)
JPEG2000
Relative energy concentration
SPIHT

ABSTRACT

In this paper, we study various lossless compression techniques for electroencephalograph (EEG) signals. We discuss a computationally simple pre-processing technique, where EEG signal is arranged in the form of a matrix (2-D) before compression. We discuss a two-stage coder to compress the EEG matrix, with a lossy coding layer (SPIHT) and residual coding layer (arithmetic coding). This coder is optimally tuned to utilize the source memory and the *i.i.d.* nature of the residual. We also investigate and compare EEG compression with other schemes such as JPEG2000 image compression standard, predictive coding based *shorten*, and simple entropy coding. The compression algorithms are tested with University of Bonn database and Physiobank Motor/Mental Imagery database. 2-D based compression schemes yielded higher lossless compression compared to the standard vector-based compression, predictive and entropy coding schemes. The use of pre-processing technique resulted in 6% improvement, and the two-stage coder yielded a further improvement of 3% in compression performance.

1. Introduction

Electroencephalogram (EEG) is a record of electrical activity of the brain. EEG provides a large-scale and robust measure of the dynamic activity of brain; it has high temporal resolution but poor spatial resolution. Though, EEG is considered as a valuable source for understanding neuronal functions and neurophysiological properties of human brain. EEG is used successfully for diagnosing brain disorders (e.g., Alzheimer's disease [1]), in sleep studies, monitoring depth of anesthesia, and in cognitive studies [2].

Various clinical applications require acquisition, archiving, transmission and automatic processing of EEG over an extended duration (several days, weeks, or potentially even months). Such long-term recordings results in massive EEG data sets. For instance, accurate inverse modeling demands the use of higher number of EEG channels (e.g., 256), and higher sampling rate may be required (several kHz in the case of cortical EEG; several hundred Hz for scalp EEG), to capture spikes and high-frequency oscillations in the EEG. On the other hand, the number of patients with neurological disorders is increasing, and hence this put forward the need for efficient and flexible compression techniques.

Signal compression is achieved by exploiting correlations in the source. The compressibility of the signal is dependant on the amplitude distribution of the signal and the power spectrum of the signal. For instance, if a single value dominates the amplitude distribution, or a single frequency dominates the power spectrum, then the signal is highly compressible. The amplitude distribution and spectral distribution of a segment of EEG is shown in Fig. 1.

Usually, the amplitude of EEG signal is very low (few μV), and the acquisition systems amplify the signal more than a million times. This leads to amplification of noise as well. This inherent noise makes the compression difficult, and poses a hindrance in achieving good compression performance.

There are three types of correlations in a multi-channel EEG signal

1. Intra-channel correlation among the adjacent samples of the signal from the same channel.
2. Inter-channel correlation among the samples acquired at the same instant of time over all the channels.
3. The brain rhythms (e.g., alpha-rhythm) also introduce correlations in EEG, but they fluctuate with time.

We briefly review the EEG compression literature in the following groups: (i) predictive schemes, (ii) transform based schemes, (iii) multichannel schemes.

1.1. Predictive schemes

EEG signal is often modeled by an auto-regressive (AR) process. AR predictor predicts the current sample as a weighted sum of previous samples. To achieve perfect reconstruction, the resid-

* Corresponding author at: Biomedical Engineering Group, Department of Applied Mechanics, IIT Madras, Chennai, Tamil Nadu 600036, India.
E-mail address: srinivasan.sivam@gmail.com (K. Srinivasan).

1746-8094/$ – see front matter © 2011 Elsevier Ltd. All rights reserved.
doi:10.1016/j.bspc.2011.01.004

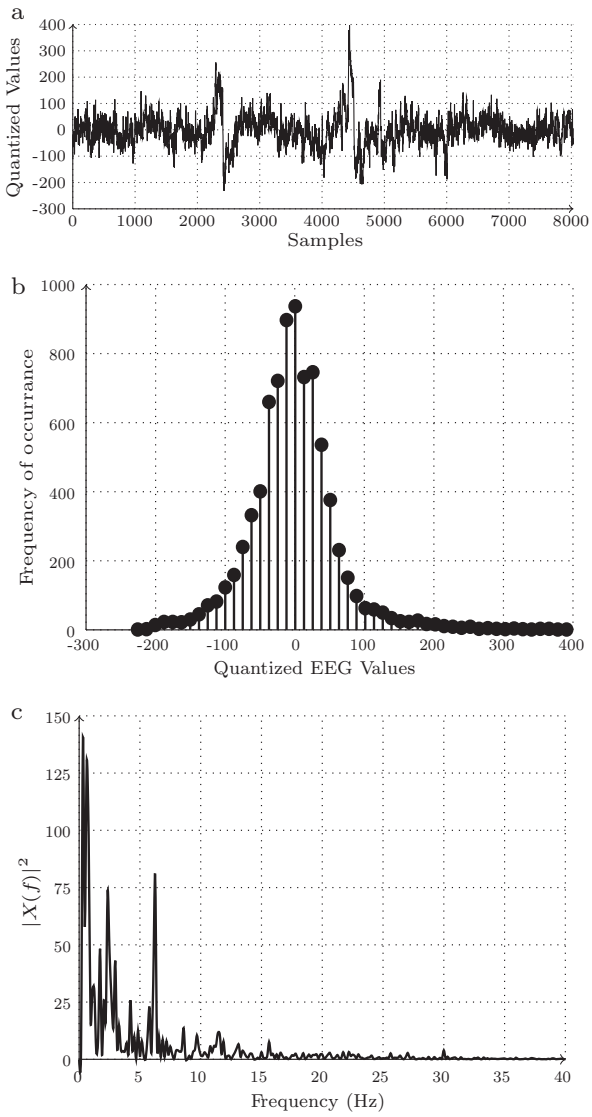

Fig. 1. Compressibility of EEG. (a) EEG signal, (b) amplitude spectra, and (c) power spectra of the signal shown in (a).

ual signal is transmitted together with the predictor coefficients. Lossless predictive schemes directly code the residuals, whereas lossy predictive schemes threshold and quantize the residuals to improve compression rate (at the cost of increased error). Various prediction models have been developed: this include linear AR model [3,4], recursive-least-squares predictor [5], adaptive neural networks [6] and models based on chaos theory [7]. Refinements such as context-based bias cancellation [4], and adaptive error modeling schemes [8,9] further improve the performance.

1.2. Transform based schemes

Consider a sequence of N signal samples X, as a N-dimensional vector. A compact representation Y in the transform domain is obtained by orthogonal transformation, $Y = TX$, where T denotes the transformation matrix. In lossy compression, M most significant components are selected such that $M \ll N$, whereas the residual signal (signal corresponding to remaining N–M transform domain coefficients) is also coded for lossless compression. The key idea is to exploit the properties of the transform domain elements (Y) such as sparsity, regularity, to form a compact code. Transforms applied include discrete cosine transform [3], sub-band transformation [10], wavelet-packet transform [11], and integer lifting wavelet transform [12,13].

1.3. Multichannel compression schemes

Predictive and transform based compression schemes operate naively on EEG signals without using any domain-specific knowledge. EEG signals recorded from spatially adjacent channels possess a high degree of correlation, which can be used to design efficient compression techniques. Techniques proposed to compress multi-channel EEG include graph-theoretic based approach [14], Karhunen–Loeve transform [15], exogenous input model [16] and vector quantization [3].

Apart from the above-mentioned EEG compression schemes, some ad hoc methods also have been designed for EEG compression: genetic algorithm based fractal EEG coding [17], EEG approximation by extracting patterns (classified signature and envelope set) [18]. The emerging field of compressed sensing opens the way to acquire signals with very few random measurements (compression while sensing), well below the Nyquist rate. For acquiring signals with compressed sensing, the signals need to be sparse in some domain (e.g., time–frequency domain). Some studies used compressed sensing and finite rate of innovation techniques to compress EEG [19,20].

Lossless compression techniques compress the signal by removing redundancies, while allowing perfect reconstruction of the original signal waveform. In lossless predictive coding, the residuals are also coded along with the predictive coefficients. In lossless transform coding, integer transforms are selected to ensure perfect reconstruction. Antoniol and Tonella [3] presented an excellent survey of lossless EEG compression techniques such as predictive coding, transform coding and vector quantization schemes. Lossless compression schemes often registers low compression performance compared to lossy compression, because of the inherent noise in the signal. This noise have no or very less correlation that could be exploited by the compression algorithms; in lossy compression this noise is removed to improve performance, but lossless compression schemes attempts to model this residual noise. Many schemes attempt to improve the lossless compression performance by modeling the residuals; this includes context-based bias cancellation [4] and detailed prediction residual modeling [8].

Here, we propose to utilize any inherent correlations in EEG to improve the lossless compression performance, by arranging the EEG in matrix form. In our previous work [21], we studied the Rate–Distortion (R–D) performance of two variants of an EEG compression algorithm; first one operates on the EEG arranged in the standard vector form (1-D), whereas the second variant arranges EEG in matrix form (2-D) before compression. The 2-D based compression algorithm gave substantial reduction in the distortion at low bit rates compared to the 1-D scheme. In addition, 2-D based scheme also improved the lossless compression as well. In this paper, we systematically explore the following: how to arrange EEG signal in matrix, the amount of smoothness of this matrix in time domain and transform domain (wavelet transform), and compression of this matrix with a two-stage compression scheme. We also compress EEG using JPEG2000, well-known image compression standard, lossless predictive coding (*shorten*) and entropy coding. We will show that the 2-D based schemes achieve higher performance compared to the other above-mentioned schemes.

The paper is structured as follows: In Section 2, we explain the arrangement of EEG signal in matrix form, and we analyze its smoothness in time and wavelet transform domain. In Section 3, we explain the two-stage compression scheme and the optimal lossy layer bit rate selection; we also present a brief outline of the other lossless compression schemes here. We discuss the experimental

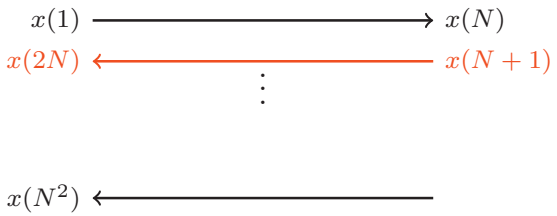

Fig. 2. Pre-processing technique: arranging the 1-D EEG signal in the form of matrix ($N \times N$). The first segment $x(1)$ to $x(N)$ is filled in the first row, and the second segment $x(N+1)$ to $x(2N)$ is arranged in the reverse fashion, as indicated by the direction of the arrow.

results in Section 4. We offer concluding remarks and some future directions in Section 5.

2. Pre-processing technique

A majority of biomedical signals is quasi-periodic, and this domain-specific knowledge can be used to improve compression performance. For example, electrocardiogram (ECG) signal is quasi-periodic i.e., the successive beats have the same structural form; when these beats are arranged in the form of a 2-D array, the correlation among the beats can be exploited effectively with a 2-D based compression scheme. This lies at the heart of a whole line of 2-D based ECG compression algorithms [22–27]. On the other hand, EEG is a slowly varying signal [3]: rhythms and periodic patterns occasionally occur depending on the state of the brain. First, we subject EEG to backward difference to remove the DC component. Then, EEG signal is arranged in the matrix form, as explained in detail below.

2.1. Proposed technique

We arrange EEG signal in the form of matrix of size $N \times N$ as shown in Fig. 2. Since EEG signal is slowly varying and contains rhythms [3], the matrix entries are correlated; the higher the above said factors, higher will be the smoothness of the matrix. The EEG signal which is cut into segments of length N are arranged as rows to form a matrix. Odd rows are filled directly, whereas even rows are filled in reverse fashion, to utilize the adjacent sample correlation. We study the smoothness of the matrix in time domain and wavelet transform domain in Sections 2.2 and 2.3 respectively.

2.2. Smoothness measure in time domain

We quantify the "Smoothness" of the matrix by means of the Pearson's correlation coefficient. The amount of smoothness is the average value of the Pearson's correlation coefficient computed for all the adjacent row pairs of the matrix ($N-1$ adjacent row pairs for a matrix with N rows).

The normalized correlation (CC_k), between two adjacent row vectors $\mathbf{X}$ and $\mathbf{Y}$ is defined as,

$$CC_k(\mathbf{X},\mathbf{Y}) = \frac{\sum_{i=1}^{N}(x_i-\hat{x})(y_i-\hat{y})}{\sqrt{\sum_{i=1}^{N}(x_i-\hat{x})^2}\sqrt{\sum_{i=1}^{N}(y_i-\hat{y})^2}} \quad k = 1, \ldots, N-1 \quad (1)$$

where CC_k represents the normalized correlation between the rows k and $k+1$, $\hat{x}$ and $\hat{y}$ represent mean of vectors $\mathbf{X}$ and $\mathbf{Y}$ respectively.

The smoothness measure of the matrix (r) in time domain, is defined as the average of the normalized correlation coefficient of all adjacent row pairs of the matrix, given by the following equation,

$$r = \frac{1}{N-1}\sum_{k=1}^{N-1} CC_k \quad (2)$$

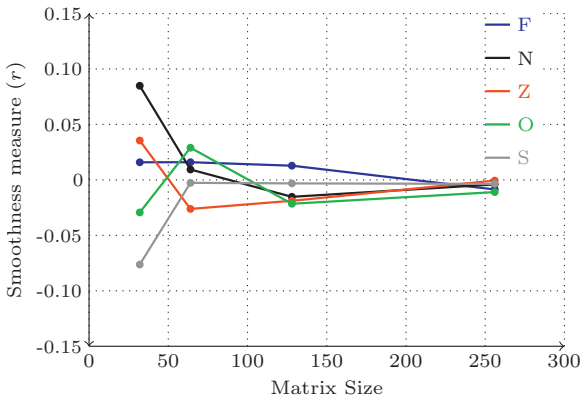

Fig. 3. Smoothness measure (r) variation with the matrix size. F, N, O, S, and Z are labels given to recordings containing normal and epileptic EEG data (dataset explanation in Section 4.1).

2.2.1. Experimental observations

The smoothness measure (r) is computed for various matrix sizes and the results are given in Fig. 3. The smoothness measure decays with increasing size of matrix; the smoothness is higher for smaller matrix sizes, and decays down to zero for matrices of larger size. This shows that the EEG signal is having a short-term memory, and this memory reflects the inherent hidden correlations in EEG; this can be utilized to improve the compression performance.

2.3. Smoothness in transform domain

2.3.1. Lifting scheme

A wavelet transform decomposes a given signal into different frequency bands; it allows to represent the signal in multiple resolutions (coarse to fine) [29]. Wavelets are usually realized by a set of filters, operating in parallel ("filter banks"). An alternative method of realizing wavelets is *lifting scheme* [30], which consists of a cascade of simple filters; it may be viewed as the factorization of a filter bank into elementary filters. One such simple filter is depicted in Fig. 4(a) and (b). The former shows the forward lifting transformation; the signal x is first split into *odd* and *even* phases x_0 and x_e respectively, containing the odd and even samples respectively of

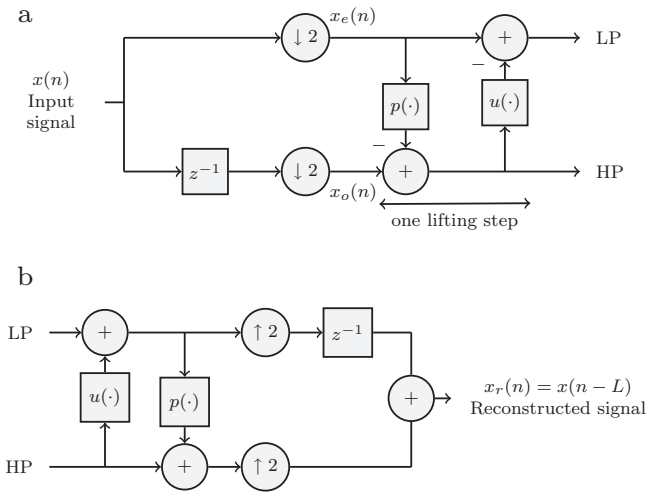

Fig. 4. Wavelet transform realization via lifting scheme. (a) forward transformation, (b) inverse transformation. The boxes labeled by z^{-1} stand for delays over one sample. The boxes $\downarrow 2$ and $\uparrow 2$ represent downsampling and upsampling respectively by a factor of two; in the latter a zero is inserted after every sample, whereas in the former, every second sample is removed. The lifting scheme repeats two primitive steps: prediction p and update u.

Table 1
Bi-orthogonal 5/3 and 9/7 integer transforms. The input signal, lowpass subband signal, and highpass subband signal are denoted by $x[n]$, $s[n]$, and $d[n]$, respectively; we consider $s_0[n] = x[2n]$ and $d_0[n] = x[2n+1]$. Lifting steps of forward transforms are listed here. Inverse transform is obtained by reversing the steps and flipping signs.

Transform	Lifting steps	Computational complexity		
		Bit-shifts	Additions	Multiplies
5/3 [28]	$d[n] = d_0[n] - \lfloor \frac{1}{2}(s_0[n+1] + s_0[n]) \rfloor$ $s[n] = s_0[n] + \lfloor \frac{1}{4}(d[n] + d[n-1]) + \frac{1}{2} \rfloor$	2	5	0
9/7 [28]	$d_1[n] = d_0[n] + \lfloor \frac{1}{128}(203(-s_0[n+1] - s_0[n])) + \frac{1}{2} \rfloor$ $s_1[n] = s_0[n] + \lfloor \frac{1}{4096}(217(-d_1[n] - d_1[n-1])) + \frac{1}{2} \rfloor$ $d[n] = d_1[n] + \lfloor \frac{1}{128}(113(s_1[n+1] - s_1[n])) + \frac{1}{2} \rfloor$ $s[n] = s_1[n] + \lfloor \frac{1}{4096}(1817(d_1[n] + d_1[n-1])) + \frac{1}{2} \rfloor$	4	12	4

input signal x. The odd and even phases contain adjacent samples; in natural signals such as EEG, adjacent samples are highly correlated. Therefore, the odd phase may be predicted from the even phase (and vice versa). By subtracting the prediction $\hat{x}_o = p(x_e)$ from the odd phase, we are left with a high-frequency residue signal (HF) of the odd phase. The latter is used in another lifting step, to predict the even phase x_e ("update" u); the resulting prediction is subtracted from the even phase x_e, which leaves the low-frequency component (LF) of the even phase x_e; this also ensures the complete frequency separation between a LF and HF components. The forward transform of Fig. 4(a) is easily invertible by reversing the steps and flipping the signs (see Fig. 4(b)).

In a lifting scheme, the pair of lifting steps, i.e., prediction p and update u, is repeated several times, leading to multi-scale representation of the input signal x ("wavelet"); the nature and number of lifting steps p and u depends on the type of wavelets [30]. Integer wavelet transforms can easily be realized by systematic rounding and truncation of the intermediate results, i.e., output of p and u [28]. Integer transforms are the key to realize lossless compression, but they have the following drawbacks: (i) relative energy concentration is poor compared to its floating-point counterpart, due to the truncation and quantization in the intermediate steps, (ii) reduced R–D performance of the coder employing integer lifting transform [21].

2.3.2. Choosing wavelet filters

Natural images/signals often have slow variations, and hence have a fair amount of low frequency content; in this case, wavelet filters with a large number of taps decorrelate well. For images with relatively greater amount of high-frequency content, wavelet filters with less number of taps performs better [31]. Here, we select two widely used wavelet filters in image compression: bi-orthogonal 9/7 and 5/3 filter. Referring Table 1, 5/3 filter has less computational complexity compared to 9/7 filter and the integer version of the 5/3 filter can be realized only using additions and bit-shifts. Moreover, the 5/3 filter have less high-pass channel growth compared to 9/7 filter, which is an essential feature, when the image/signal is having relatively large high-frequency content [31].

2.3.3. Energy compaction efficiency (ECE)

As discussed in Section 2.3.2, the amount energy concentrated in the low frequency bands is a measure of signal's smoothness; here, we consider the relative energy concentration (compared to total energy) as an indicator of smoothness. One level of wavelet decomposition of the matrix produces an approximate subband (low frequency (LF) band) and three high frequency (HF) subbands namely horizontal, vertical, and diagonal (H, D and V) bands (Fig. 6). These H, D and V bands carry HF information along the horizontal, vertical and diagonal direction of the matrix. When more energy is concentrated in the LF band compared to HF bands, then the matrix is considered smooth, with the amount of smoothness proportional to the energy concentration in LF band. We call the relative energy concentration in each subband as energy compaction efficiency of the particular subband.

For J-level wavelet decomposition, ECE is computed as follows,

$$ECE_{D_i} = \frac{E_i^h + E_i^v + E_i^d}{\text{Total energy}} \times 100, \quad 1 \le i \le J \tag{3}$$

$$ECE_A = \frac{E_A}{\text{Total energy}} \times 100 \tag{4}$$

where, E_i^h, E_i^v, E_i^d is the energy of the horizontal, vertical, and diagonal subbands at decomposition level i respectively; E_A is the energy of the approximate subband; ECE_{D_i} is energy compaction efficiency of the HF subbands (H, V and D) at decomposition level i; ECE_A is energy compaction efficiency of the LF subband (A) at decomposition level J; J is maximum number of wavelet decomposition levels.

For efficient compression with wavelet based compression schemes (e.g., SPIHT), the wavelet subbands must satisfy the following property, known as monotone spectral ordering [32]:

$$ECE_{D_{i+1}} > ECE_{D_i} \quad \forall i = 1, \ldots, J-1 \tag{5}$$

$$ECE_A > ECE_{D_i} \quad \forall i \le J \tag{6}$$

The above equations state that the energy in the low frequency band must be higher compared to the high frequency bands. If this condition is satisfied, then the wavelet coefficients at low frequencies have high magnitude and this magnitude decays with increasing frequency. Hence, tree-based sets (Fig. 6) originating at low-frequencies and branching towards high frequencies can be used to efficiently represent the data; at a particular threshold, if the root node is significant and all its child and grand children are insignificant, then such tree is called as a zero-tree. A large number of zero-trees give high compression efficiency. It is very difficult to satisfy the monotone spectral ordering conditions for every matrix formed from EEG, however, this criteria is important for selecting wavelet filter.

2.3.4. Experimental observations

We summarize the energy compaction efficiency for a EEG matrix in Fig. 5. We use a three-level wavelet decomposition on a EEG matrix of size 64×64; the results for both 5/3 and 9/7 integer wavelet filters are given. Fig. 5(a) gives the relative energy concentration (ECE) in subbands at each level of decomposition. Fig. 5(b) gives the variation of the energy concentration in LF approximation band (ECE_A)) with increasing matrix size. We observe the following:

1. The relative performance of the 5/3 filter is better compared to the 9/7 filter, though both of them does not satisfy the monotone spectral ordering conditions (5) and (6).
2. There is no much improvement in the energy compaction in LF band (ECE_A) with increase in matrix size. Hence, we can expect small or no improvement in compression performance for larger matrix sizes.

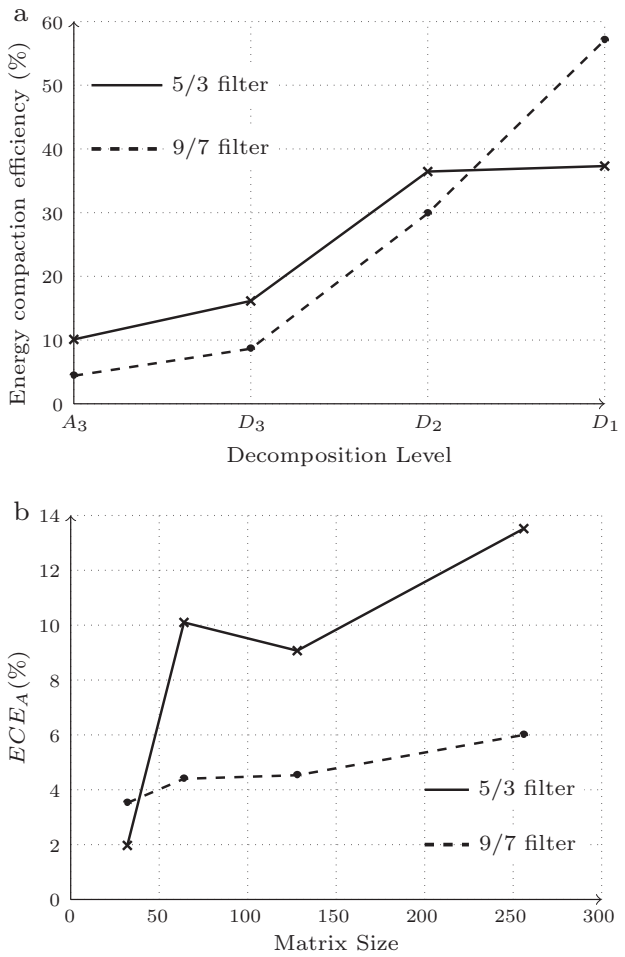

Fig. 5. Selection of wavelet filter based on energy compaction efficiency. (a) Energy compaction efficiency (%) for a three level decomposition. (b) Variation of energy concentration in the low-frequency band (ECE_A) with the matrix size.

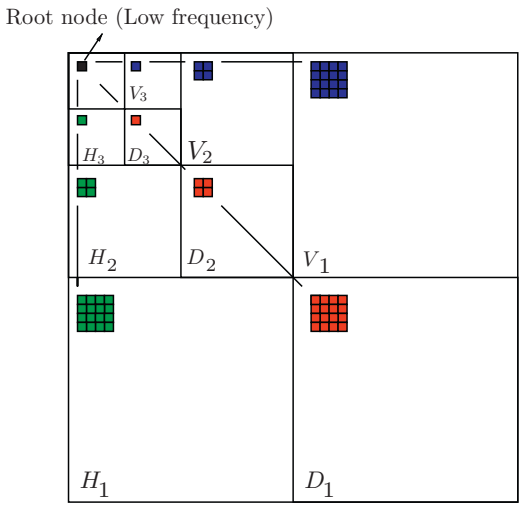

Fig. 6. Subband structure and tree-based sets. Subband structure for a three level wavelet decomposition is shown here. A, H, V and D represents the approximate (LF), horizontal, vertical and diagonal subbands and subscripts indicate the level of decomposition. The tree-based set is also shown, which originates at the root node (black) and branches successively towards the high-frequency bands (H, V and D).

Table 2
Relative energy concentration along different orientations. Distribution of energy in the approximate (LF), horizontal, vertical and diagonal HF subbands.

Band	Relative energy concentration (%)	
	9/7 filter	5/3 filter
Approximate	4.40	10.10
Horizontal	54.68	53.57
Diagonal	20.68	15.97
Vertical	20.23	20.36

On the other hand, we also study the amount of energy concentration along different orientations (H, V, and D). Interestingly, Table 2 shows that nearly 50% of the total energy is concentrated in horizontal HF bands. Relatively, 5/3 filter performed better compared to 9/7 filter, with the better performance of comes due to the short-term memory of EEG.

3. Compression algorithm

A diagram of the proposed lossless EEG compression scheme is depicted in Fig. 7. The EEG signal is arranged in matrix form before applying the 2-D compression scheme; in principle, any image compression scheme can be chosen. As our primary coder, we choose a two-stage coding scheme (Fig. 8), with SPIHT in the first stage (lossy-coding stage) until an optimal rate, and arithmetic coding for encoding the residuals. For comparison, we choose JPEG2000, a widely used compression algorithm for image compression, a lossless linear prediction scheme (*shorten*), and a single-context arithmetic coding. We discuss these algorithms in the following sections.

3.1. Set partitioning based two-stage coder (SPIHT + AC)

Set partitioning in hierarchical trees (SPIHT) is a widely used algorithm for image coding, which works by forming, partitioning of sets guided by a series of threshold tests [33]. This algorithm works on transform domain (e.g., wavelet transform), as magnitude of the transform domain coefficients tend to have close values compared to raw data. In SPIHT, tree-based non-overlapping sets are formed from the wavelet transform coefficients, rooted at low-frequency band and branch successively to high-frequency bands at the same spatial location (Fig. 6).

Fig. 8 shows the schematic of the two-stage coder. SPIHT is used in the first stage as a lossy-coding layer, which encodes the wavelet coefficients until a bit rate, and then wavelet domain residuals are encoded by single context arithmetic coding. This produces a bit-stream S_{enc} from the SPIHT coding stage, and R_{enc} from the residual coding.

From the well-known principles of R–D theory, when the bit rate for the lossy reconstruction of the source becomes larger than "critical-rate" (R_0), then the encoding residual of a source becomes identically and independently distributed (*i.i.d.*) Gaussian under mean-squared error distortion measure [34]. Hence, when the SPIHT encoding is done until R_0, the encoding source lose its memory and behave *i.i.d.* that a good lossy-coder can take advantage of, so the coding efficiency of such coder tends to worse than that of entropy coding. The selection of optimal bit rate R_0 is very important to achieve a good compression performance, as complete advantage can be taken over the memory of the source and the *i.i.d.* residual as well.

We analyze the total bit rate and residual bit rate variation with the lossy-layer bit rate; this give an idea about the optimal rate for the source (EEG matrix) used here. We summarize the results in Fig. 9. Fig. 9(a) shows that the residual bit rate is monotonously decreasing, whereas the total bit rate decreases until a bit-rate and

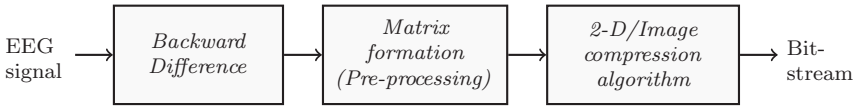

Fig. 7. General schematic of 2-D based EEG signal compression.

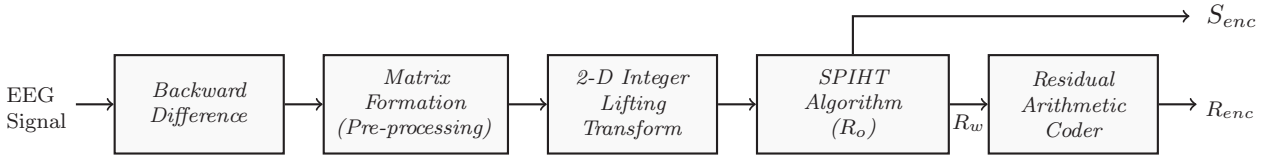

Fig. 8. Two-stage coder for EEG compression: first lossy-stage is SPIHT encoder until an optimal rate (R_0), followed by arithmetic coding for residuals.

then starts increasing. As we discussed in the previous paragraph, this bit rate is called as optimal bit rate (R_0), where the encoding source turns *i.i.d.* The magnified graphs of the total bit rate curves in Fig. 9(b) shows the existence of the optimal rate; the slope of the total bit rate curve is very small, which indicates the short-term memory of the EEG matrix. Fig. 9 shows that all the matrix sizes behave similarly, and there is no much variation in the slope or the optimal rate. The increase in total bit rate after R_0 shows the inefficiency of SPIHT, and hence we use a single-context arithmetic coder for encoding residuals.

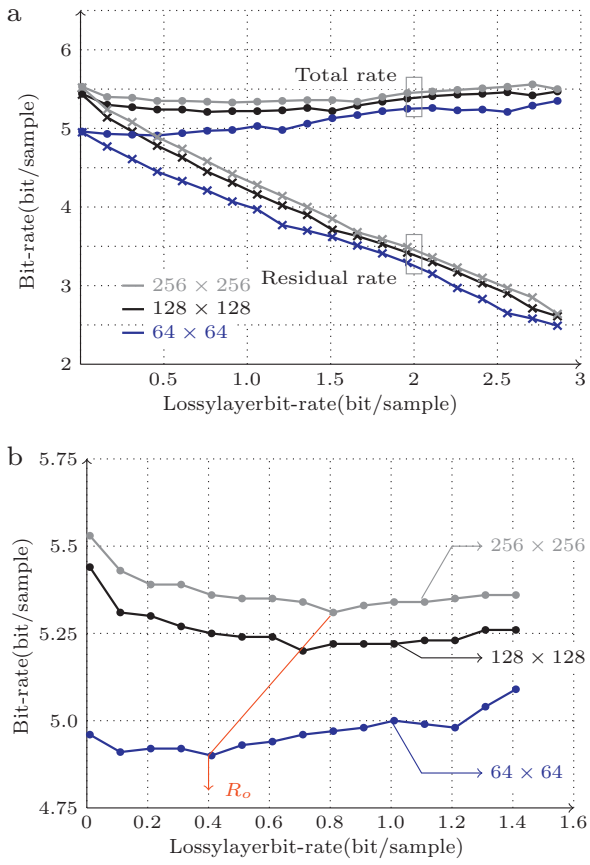

Fig. 9. Optimal bit rate determination for the EEG matrix. (a) Bit rates (total and residual bit rate variations). (b) Total bit rate variation (magnified graph of (a)). Optimal bit rate for EEG matrix of different sizes are indicated using a red line. (For interpretation of the references to color in this figure legend, the reader is referred to the web version of the article.)

3.2. JPEG2000 in lossless mode (JPEG2000LS)

JPEG2000 is a widely used wavelet-based still-image compression standard. The image to be coded is split into non-overlapping rectangular tiles; each tile is subjected to wavelet transform followed by a quantizer and bit plane coder. For lossless compression, integer wavelet transform is chosen and quantizer step size is set to one. Adaptive arithmetic coder and the bit-stream organizer comprise the bit-plane coder. JPEG2000 produces an embedded bit-stream, which can be terminated at any instant to reconstruct signal with minimum mean-squared error. The bit-stream generated by JPEG2000 has many desirable properties such as resolution scalability and signal-to-noise ratio scalability. Explanation of JPEG2000 is beyond the scope of this article, and we refer to [35] for more details.

3.3. Shorten

The lossless predictive coding algorithm used here is called *shorten*, which use a linear predictor to remove temporal correlation and Huffman coding for encoding residuals [36]. Residuals are assumed to follow Laplacian distribution and Huffman code is assigned based on a efficient and simple method. We used a sixth-order linear predictor, as it is widely used in previous EEG compression study [4].

3.4. Arithmetic coding (AC)

Arithmetic coding is a widely used entropy coding scheme, which gives optimal compression for *i.i.d.* sources. Consider a source emitting one of the N symbols with probabilities $\{p_i\}_{i=1}^{N}$. Consider a symbol sequence of length M, $S = \{s_i\}_{i=0}^{M-1}$ to be encoded; the arithmetic coding process creates a nested sequence of intervals according to the probability of the symbols in the symbol sequence S. This process results in a small interval at the end of the last symbol; this interval represents the whole symbol sequence S, and the code is formed by choosing a real number from this interval and converting it into binary form. The output code is optimal in the sense that the probability distributions of the code values are uniformly distributed in the interval [0, 1). We refer to [37] for more detailed discussions.

4. Experimental results

4.1. Datasets

We consider two EEG databases here: University of Bonn database, and Physiobank Motor/Mental Imagery (MMI) database. University of Bonn database [38] consists of five datasets, labeled F,

Table 3
Compression ratios of 2-D based compression (SPIHT + AC, JPEG2000 and 2-D SPIHT), 1-D based compression (1-D SPIHT), predictive coding (SHORTEN) and entropy coding scheme (AC) for the University of Bonn and EEG-MMI physiobank EEG databases.

Dataset	2-D based algorithms			1-D based algorithms		
	SPIHT + AC	JPEG2000	2-D SPIHT [21]	SHORTEN	AC	1-D SPIHT [21]
F	**2.19**	2.13	2.18	1.34	1.51	2.02
N	**2.23**	2.15	2.15	1.27	1.55	1.99
O	1.84	**1.87**	1.86	1.24	1.46	1.77
S	1.44	**1.48**	1.44	1.27	1.15	1.42
Z	**2.01**	1.90	1.99	1.18	1.61	1.85
S001-ec	**1.78**	1.69	1.73	1.13	1.54	1.64
S001-eo	**1.82**	1.72	1.74	1.17	1.52	1.65
S005-ec	1.49	**1.68**	1.41	1.13	1.64	1.30
S005-eo	1.50	**1.68**	1.41	1.20	1.63	1.30
S026-ec	**1.83**	1.73	1.72	1.11	1.67	1.61
S026-eo	**1.81**	1.71	1.70	1.15	1.66	1.59
Average	**1.81**	1.79	1.75	1.20	1.54	1.65

N, O, Z, and S. Each recording have 100 single-channel EEG recordings of 23.6 s duration, sampled at 173.21 Hz, and digitized at 12-bit resolution [38]. The datasets F and N contains EEG from epileptic patients measured during seizure free intervals, O and Z contains normal EEG with eyes open and closed, and S contains purely epileptic EEG.

The second dataset, MMI database are EEGs recorded from subjects performing different Motor/Mental Imagery tasks [39,40]. These recordings contains 64-channel EEGs, sampled at 80 Hz, and digitized at 12-bit resolution. EEGs are recorded in the eyes open and closed conditions, which are the baseline recordings (normal EEG) from three datasets (S001, S005 and S026).

4.2. Performance measure

We compare the performance of the different algorithms using compression ratio, the factor of reduction in file size, given by:

$$\mathrm{CR} = \frac{L_{\mathrm{orig}}}{L_{\mathrm{comp}}} \tag{7}$$

where L_{orig} and L_{comp} refer to bitstream length of the original and compressed sources respectively.

4.3. Implementation details

We use a EEG sample size of 4096 for all the compression algorithms; in 2-D based compression algorithms, we arrange these samples as a matrix of size 64×64. Bi-orthogonal 5/3 filter is used for all the wavelet based compression algorithms (SPIHT + AC, JPEG2000, 2-D SPIHT, and 1-D SPIHT). In SPIHT + AC, we set the empirically determined optimal bit rate of 0.6 bit/sample for the lossy coding layer. For *shorten*, we use linear predictor of order six.

4.4. Discussion

We present the relative performance of the 2-D and 1-D based compression algorithms in Table 3; we also include the results from our previous work on 2-D based lossless EEG compression [21]. SPIHT + AC, JPEG2000 and 2-D SPIHT are applied to EEG signal after pre processing, and hence their results are listed under the category of 2-D based compression schemes; we group all the other schemes under 1-D based compression schemes. The values given in Table 3 are average values within the particular dataset; the average CR over all the datasets is given in the last row.

Table 3 shows that 2-D based compression algorithms performed well compared to the 1-D based compression schemes. SPIHT + AC registered the best average performance compared to all other schemes; it is followed by JPEG2000, 2-D SPIHT, 1-D SPIHT, AC and *shorten*. Interestingly, the performance of *shorten* is low compared to simple entropy coding (AC). Generally, transform based coding schemes (SPIHT+AC, JPEG2000, 2-D SPIHT and 1-D SPIHT) performed better compared to the predictive based *shorten* and arithmetic coding.

The average CR of the 2-D SPIHT is 6% higher than 1-D SPIHT; the primary difference between the above two compression algorithm is that the former is applied to EEG arranged in matrix form, whereas the latter is applied to EEG in vector form (1-D). Hence, the amount of improvement is due to the arrangement of EEG in matrix form. Next, SPIHT + AC register 3.2% improvement over 2-D SPIHT; this improvement is due to optimal use of source memory using SPIHT, and the *i.i.d.* residual using entropy coding scheme. Thus, arranging the EEG in the form of matrix and use of two-stage coding scheme led to improvement of lossless compression performance by nearly 9%.

4.4.1. Limitations

We observe a marginal improvement in compression performance with the pre-processing technique; this is mainly due to the following limitations. First, EEG is a non-stationary signal, and this affects the smoothness of the matrix and cause the average compression performance to reduce. Second, the 2-D based compression algorithms used for compression of EEG matrix are designed for natural images, which is smoother compared to EEG matrix. The first limitation is due to the inherent nature of signal, whereas the second limitation can be handled by modifying the compression algorithm to suit the source characteristics (EEG matrix).

5. Conclusion

In this paper, we discussed a novel and simple pre-processing scheme of arranging EEG in matrix form before compression. This opens the way to realize EEG compression with image compression techniques. We proposed a two-stage coding scheme consisting of a lossy coding layer and a residual coding layer. We compared the result of this two-stage coding with JPEG2000, *shorten* and arithmetic coding. A marginal improvement could be obtained with the use of two-stage coder, which is owed to the use of pre-processing technique and the optimal use of memory in the EEG matrix.

The 2-D compression schemes employed here are particularly designed for compression of the natural images, whose statistics are entirely different from that of EEG matrix. Hence, as a future expansion, custom compression schemes need to be devised for improved lossless compression performance.

Acknowledgements

The authors would like to thank Dr. R.G. Andrzejak of University of Bonn, Germany for providing us with the datasets, and Dr. N.

Sriraam of SSN College of Engineering, Chennai, India for his help and suggestions. Two anonymous reviewers are greatly thanked for their very thorough and inspiring review, which substantially improved the manuscript.

References

[1] J. Dauwels, F. Vialatte, A. Cichocki, Diagnosis of alzheimers disease from EEG signals: where are we standing? Current Alzheimer Research 7 (2010) 487–505.
[2] P.L. Nunez, R. Srinivasan, Electric Fields of Brain, 2nd ed., Oxford University Press, 2006.
[3] G. Antoniol, P. Tonella, EEG data compression techniques, IEEE Transactions on Biomedical Engineering 44 (2) (1997) 105–114.
[4] N. Memon, X. Kong, J. Cinkler, Context-based lossless and near-lossless compression of EEG signals, IEEE Transactions on Biomedical Engineering 3 (3) (1999) 231–238.
[5] N. Magotra, G. Mandyam, M. Sun, W. McCoy, Lossless compression of electroencephalographic (EEG) data, IEEE International Symposium on Circuits and Systems 2 (1996) 313–315.
[6] N. Sriraam, C. Eswaran, Performance evaluation of neural network and linear predictors for near-lossless compression of EEG signals, IEEE Transactions on Information Technology in Biomedicine 12 (1) (2008) 87–93.
[7] V. Kavitha, D. Narayana Dutt, Use of chaotic modeling for transmission of EEG data, International Conference on Information, Communications and Signal Processing (ICICS) Vol.3 (1997) 1262–1265.
[8] N. Sriraam, C. Eswaran, An adaptive error modeling scheme for the lossless compression of EEG signals, IEEE Transactions on Information Technology in Biomedicine 12 (5) (2008) 587–594.
[9] N. Sriraam, C. Eswaran, Context based error modeling for lossless compression of EEG signals using neural networks, Journal of Medical Systems 30 (2006) 439–448.
[10] Z. Sijerčić, G. Agarwal, Tree structured filter bank for time-frequency decomposition of EEG signals, IEEE 17th Annual Conference Engineering in Medicine and Biology Society 2 (1995) 991–992.
[11] J.L. Cárdenas-Barrera, J.V. Lorenzo-Ginori, E. Rodríguez-Valdivia, A wavelet-packet based algorithm for EEG signal compression, Informatics for Health and Social Care 29 (1) (2004) 15–27.
[12] M. Sun, Q. Liu, K.C. Yi, C.-C. Li, R. Sclabassi, Fast internet transmission of physiological signals using the lifting scheme and SPIHT coding algorithm, 6th International Conference on Signal Processing 2 (2002) 1544–1547.
[13] K. Srinivasan, M.R. Reddy, Selection of optimal wavelet for lossless EEG compression for real-time applications, in: 2nd National Conference on Biomechanics, IIT Roorkee, India, 2009.
[14] Q. Liu, M. Sun, R. Sclabassi, Decorrelation of multichannel EEG based on hjorth filter and graph theory, 6th International Conference on Signal Processing 2 (2002) 1516–1519.
[15] Y. Wongsawat, S. Oraintara, T. Tanaka, K. Rao, Lossless multi-channel EEG compression, Proceedings of IEEE International Symposium on Circuits and Systems (ISCAS) (2006) 1611–1614.
[16] D. Gopikrishna, A. Makur, A high performance scheme for EEG compression using a multichannel model, in: High Performance Computing HiPC 2002, Lecture Notes in Computer Science, vol. 2552, Springer, Berlin/Heidelberg, 2002, pp. 443–451.
[17] S.K. Mitra, S.N. Sarbhadhikari, Iterative system function and genetic algorithm based EEG compression, Medical Engineering & Physics 19 (7) (1997) 605–617.
[18] H. Gürkan, U. Guz, B.S. Yarman, EEG signal compression based on classified signature and envelope vector sets, International Journal of Circuit Theory and Applications 37 (2) (2009) 351–363.
[19] S. Aviyente, Compressed sensing framework for EEG compression, in: IEEE/SP 14th Workshop on Statistical Signal Processing (SSP), 2007, pp. 181–184.
[20] K.-K. Poh, P. Marziliano, Compressive sampling of EEG signals with finite rate of innovation, EURASIP Journal on Advances in Signal Processing 2010 (2010) 1–12.
[21] K. Srinivasan, M.R. Reddy, Efficient pre-processing technique for lossless real-time EEG compression, Electronics Letters 46 (1) (2010) 26–27.
[22] H. Lee, K.M. Buckley, ECG data compression using cut and align beats approach and 2-D transforms, IEEE Transactions on Biomedical Engineering 46 (5) (1999) 556–564.
[23] J.-J. Wei, C.-J. Chang, N.-K. Chou, G.-J. Jan, ECG data compression using truncated singular value decomposition, IEEE Transactions on Information Technology in Biomedicine 5 (4) (2001) 290–299.
[24] A. Bilgin, M.W. Marcellin, M.I. Altbach, Compression of electrocardiogram signals using JPEG2000, IEEE Transactions on Consumer Electronics 49 (4) (2003) 833–840.
[25] S.-C. Tai, C.-C. Sun, W.-C. Yan, A 2-D ECG compression algorithm based on wavelet transform and modified SPIHT, IEEE Transactions on Biomedical Engineering 52 (6) (2005) 999–1008.
[26] H.-H. Chou, Y.-J. Chen, Y.-C. Shiau, T.-S. Kuo, An effective and efficient compression algorithm for ECG signals with irregular periods, IEEE Transactions on Biomedical Engineering 53 (6) (2006) 1198–1205.
[27] X. Wang, J. Meng, A 2-D ECG compression algorithm based on wavelet transform and vector quantization, Digital Signal Processing 18 (2008) 179–188.
[28] R. Calderbank, I. Daubechies, W. Sweldens, B.-L. Yeo, Wavelet transforms that map integers to integers, Applied and Computational Harmonic Analysis 5 (3) (1998) 332–369.
[29] S.G. Mallat, A theory for multiresolution signal decomposition:the wavelet representation, IEEE Transactions Pattern Analysis and Machine Intelligence 2 (7) (1989) 674–693.
[30] I. Daubechies, W. Sweldens, Factoring wavelet transforms into lifting steps, Journal of Fourier Analysis and Applications 4 (3) (1998) 245–267.
[31] M.D. Adams, F. Kossentini, Reversible integer-to-integer wavelet transforms for image compression: performance evaluation and analysis, IEEE Transactions on Image Processing 9 (6) (2000) 1010–1024.
[32] V.N. Ramaswamy, N. Ranganathan, K.R. Namuduri, Performance analysis of wavelets in embedded zero-tree based lossless image coding schemes, IEEE Transactions on Signal Processing 43 (3) (1999) 884–889.
[33] A. Said, W.A. Pearlman, A new, fast and efficient image codec based on set paritition in hierarchial trees, IEEE Transactions on Circuits and Systems for Video Technology 6 (3) (1996) 243–250.
[34] S Yea, W. Pearlman, A wavelet-based two stage near lossless coder, IEEE Transactions on Image Processing 15 (11) (2006) 3488–3500.
[35] M. Rabbani, R. Joshi, An overview of JPEG 2000 still image compression standard, Signal Processing: Image Communications 17 (2002) 3–48.
[36] T. Robinson, SHORTEN: simple lossless and near-lossless waveform compression, Tech. rep. cued/f-infeng/tr.156, Cambridge University, Engineering Department, Trumpington Street, Cambridge, CB2 1PZ, UK (Dec. 1994).
[37] K. Sayood, Lossless Compression Handbook, Academic Press, 2003, Ch. 5 – Arithmetic Coding, pp. 101–152.
[38] R.G. Andrzejak, K. Lehnertz, F. Mormann, C. Rieke, P. David, C.E. Elger, Indications of nonlinear deterministic and finite-dimensional structures in time series of brain electrical activity: dependence on recording region and brain state, Physical Review E 64 (6) (2001) 061907.
[39] G. Schalk, D.J. McFarland, T. Hinterberger, N. Birbaumer, J.R. Wolpaw, BCI2000: a general-purpose brain–computer interface (BCI) system, IEEE Transactions on Biomedical Engineering 51 (6) (2004) 1034–1043.
[40] A.L. Goldberger, L.A.N. Amaral, L. Glass, J.M. Hausdorff, P.C. Ivanov, R.G. Mark, J.E. Mietus, G.B. Moody, C.-K. Peng, H.E. Stanley, PhysioBank, PhysioToolkit, and PhysioNet: components of a new research resource for complex physiologic signals, Circulation 101 (23) (2000) e215–220.